

Geometry of high-lying eigenfunctions in a plane billiard system having mixed-type classical dynamics

This article has been downloaded from IOPscience. Please scroll down to see the full text article.

1995 J. Phys. A: Math. Gen. 28 2799

(<http://iopscience.iop.org/0305-4470/28/10/012>)

View [the table of contents for this issue](#), or go to the [journal homepage](#) for more

Download details:

IP Address: 171.66.16.68

The article was downloaded on 02/06/2010 at 00:01

Please note that [terms and conditions apply](#).

Geometry of high-lying eigenfunctions in a plane billiard system having mixed-type classical dynamics

Baowen Li† and Marko Robnik‡

Center for Applied Mathematics and Theoretical Physics, University of Maribor, Krekova 2, SLO-62000 Maribor, Slovenia

Received 14 October 1994, in final form 8 February 1995

Abstract. In this paper we study the geometrical properties of the high-lying eigenfunctions (200 000 and above) which are deep in the semiclassical regime. The system we are analysing is the billiard system inside the region defined by the quadratic (complex) conformal map $w = z + \lambda z^2$ of the unit disc $|z| \leq 1$ as introduced by Robnik (1983), with the shape parameter value $\lambda = 0.15$, so that the billiard is still convex and has KAM-type classical dynamics, where regular and irregular regions of classical motion coexist in the classical phase space. By inspecting 100 and by showing 36 consecutive numerically calculated eigenfunctions we reach the following conclusions: (i) Percival's (1973) conjectured classification in regular and irregular states works well: the mixed-type states 'living' on regular and irregular regions disappear in the semiclassical limit. (ii) The irregular (chaotic) states can be strongly localized due to the slow classical diffusion, but become fully extended in the semiclassical limit when the break time becomes sufficiently large with respect to the classical diffusion time. (iii) Almost all states can be clearly associated with some relevant classical object such as the invariant torus, cantorus or periodic orbits. This paper is largely qualitative but deep in the semiclassical limit and as such it is a prelude to our next paper which is quantitative and numerically massive but at about ten times lower energies.

1. Introduction

The stationary problem in quantum chaos comprises the statistical properties of energy spectra, the statistical properties of the matrix elements of other observables, and of geometric structure (morphology) of the eigenfunctions and their statistics. Some recent reviews are in Gutzwiller's book (1990), Giannoni *et al* (1991), Casati *et al* (1993), and also in Berry (1983). As for the energy spectra we have massive numerical and experimental evidence for the existence of universality classes of spectral fluctuations described, for example, in Robnik (1994), supplemented by heuristic and intuitive arguments as well as more rigorous approaches based on applying the trace formulae, e.g. in Berry (1985) and especially in recent works by Steiner (1994), and by Aurich *et al* (1994). In performing that kind of analysis the goodness of semiclassical approximations still has to be carefully assessed, although Prosen and Robnik (1993a) demonstrate that semiclassics will correctly describe the statistical measures especially at large energy ranges even if it fails to predict the individual energy levels. These latter works deal with completely chaotic systems (ergodic, mixing and having positive K -entropy) whilst the situation in generic KAM-like systems

† E-mail address: Baowen.Li@UNI-MB.SI

‡ E-mail address: Robnik@UNI-MB.SI

with mixed classical dynamics is much more complicated but nevertheless almost entirely understood in the recent works (Prosen and Robnik 1994a,b).

The structure and the statistical properties of the eigenfunctions are not so well understood, especially in the transition region of mixed classical dynamics, which is the subject of the present work, whereas in the two extreme cases of complete integrability on one side, and the complete ergodicity on the other side, much more is known. In our recent paper (Li and Robnik 1994a, henceforth referred to as LR) we have analysed the high-lying eigenfunctions in the completely ergodic regime and confirmed some major theoretical predictions.

In order to understand the wavefunctions especially in the semiclassical limit it is intuitively very appealing to use the so-called *principle of uniform semiclassical condensation* (PUSC) of the Wigner functions (of the eigenstates) which is implicit in Berry (1977a), Robnik (1988), and was used in LR. As $\hbar \rightarrow 0$ we assume that the Wigner function of a given eigenstate uniformly (ergodically) condenses on the classical invariant object on which the classical motion is ergodic and which supports the underlying quantal state. Such an object can be, for example, an invariant torus, a chaotic region as a proper subset of the energy surface, or the entire energy surface if the system has ergodic dynamics there.

In classically integrable systems the eigenfunctions possess a lot of ordered structure *globally* and *locally*. Applying PUSC the average probability density in the configuration space is seen to be determined by the projection of the corresponding quantized invariant torus onto the configuration space, which implies the global order. Moreover, the local structure is implied by the fact that the wavefunction in the semiclassical limit is locally a superposition of a finite number of plane waves (with the same wavenumber as determined by the classical momentum).

In the opposite extreme of a classically ergodic system PUSC predicts that the average probability density is determined by the microcanonical Wigner function (Shnirelman 1979, Berry 1977a, Voros 1979). Its local structure is spanned by the superposition of infinitely many plane waves with random phases and equal wavenumber. The random phases might be justified by the classical ergodicity and this assumption, originally due to Berry (1977b), is a good starting approximation which locally immediately predicts the Gaussian randomness for the probability amplitude distribution. One major surprise in this research was Heller's discovery (1984) of scars of unstable classical periodic orbits in classically ergodic systems. The scar phenomenon is, of course, a consequence of subtle correlations in the quantal phases. This has been analysed and discussed by Bogomolny (1988) and Berry (1989) in the context of the Gutzwiller periodic orbit theory. The insufficiency of the single-periodic-orbit theory of scars has been discussed by Prosen and Robnik (1993b) in a study of the transition region between integrability and chaos. In the latter work Prosen and Robnik have emphasized the incompleteness of the current semiclassical approximations (Gutzwiller's method and torus quantization method) in describing the individual eigenstates. Their failure to predict the individual energy levels has been demonstrated in Prosen and Robnik (1993a), see also Boasman (1994) and Szeredi *et al* (1994) for discussions and related results. See also Provost and Baranger (1993).

In the generic case of a KAM-like system with mixed classical dynamics the application of PUSC is again very useful and has a great qualitative predictive power. Here the states can be classified as either regular (they 'live' on a quantized invariant torus) or irregular (they 'live' on a chaotic invariant region), quite in agreement with Percival's (1973) speculative prediction, which has been recently carefully re-analysed by Prosen and Robnik (1994a). In this case PUSC implies asymptotic ($\hbar \rightarrow 0$) statistical independence of level series (subsequences) associated with different regular and irregular components. This picture

has been used by Berry and Robnik (1984) to deduce the resulting energy level statistics in such generic Hamilton systems with mixed classical dynamics, especially the level spacing distribution. In recent work Prosen and Robnik (1994a,b) have numerically confirmed the applicability of the Berry–Robnik theory as the asymptotically exact theory and also explained the Brody-like behaviour (as discovered and described in Prosen and Robnik (1993c)) before reaching the far semiclassical limit.

In our present paper, which is an extensive, systematic and numerically massive work, we try to phenomenologically classify the variety of eigenstates in the KAM-like regime of mixed classical dynamics. We do so in sections 3 and 4 by a survey of about 100 mostly consecutive eigenfunctions of even parity which start at about the 100 000th state, of which we show and discuss a block of 36 consecutive states in configuration and in phase space in figures 2–4. In the subsequent sections we shall illustrate, discuss and confirm the theoretical pictures outlined above. The main objective of the present paper is to perform clear classification of eigenstates at the qualitative level but conceptually precise and therefore as high as possible in the semiclassical limit, so that it can serve as a prelude to our next paper (Li and Robnik 1994c,d) where we perform an extensive and careful quantitative analysis of 4000 consecutive eigenstates (no missing states) but at ten times lower energies.

2. The billiard system and the numerical technique

The domain \mathcal{B}_λ (in w -plane) of our 2D billiard system is defined by the complex quadratic conformal map of the unit disc (in the z -plane) onto the complex w -plane, namely

$$\mathcal{B}_\lambda = \{w | w = z + \lambda z^2, |z| \leq 1\} \quad (1)$$

as introduced by Robnik (1983, 1984) and further studied by Prosen and Robnik (1993c, 1994b). See also Hayli *et al* (1987), Bruus and Stone (1994), Stone and Bruus (1993a, b) and Frisk (1990). (Most people in the field call this system a Robnik billiard, or the Robnik model.) As the shape parameter λ changes from 0 to $\frac{1}{2}$ this system goes from the integrable case of the circular billiard $\lambda = 0$ continuously through a KAM-like regime $0 < \lambda < \frac{1}{4}$ to an almost ergodic regime at larger λ , becoming rigorously ergodic at least at $\lambda = \frac{1}{2}$, where a cusp singularity appears at the boundary point $z = -1$, mapped onto $w = -1 + \lambda$, where the mapping $w = w(z)$ is then no longer conformal, since $dw/dz = 0$ there. Because the boundary is sufficiently smooth, in fact analytic for all $0 \leq \lambda < \frac{1}{2}$, the KAM theorem applies *provided* the boundary is convex. If the boundary is not convex but still analytic the KAM theory does *not* apply because the bouncing map (Poincaré map) is *not* continuous in such a billiard. At $0 \leq \lambda < \frac{1}{4}$ the boundary is convex with positive curvature everywhere and therefore the Lazutkin-like caustics and invariant tori (of boundary glancing orbits) exist, in agreement with the KAM theorem (Lazutkin 1991, 1981). If the smooth boundary of a convex plane billiard has a point of zero curvature, then it has been proven by Mather (1982, 1988) that the Lazutkin caustics and the associated invariant tori do not exist. In our billiard this happens at $\lambda = \frac{1}{4}$ for $z = -1$, i.e. $w = -1 + \lambda$. Therefore, at $\lambda \geq \frac{1}{4}$ the billiard was speculated (based on the applicability of the Mather theorem and non-applicability of the KAM-theorem and on numerical evidence in Robnik (1983)) to become ergodic, which has been disproved by Hayli *et al* (1987). Close to $\lambda \geq \frac{1}{4}$ there are still some stable periodic orbits surrounded by very tiny stability islands. On the other hand, for $\lambda = \frac{1}{2}$ (the cardioid billiard, having the above-mentioned cusp singularity) the ergodicity and mixing have been rigorously proved by Markarian (1993). See also Wojtkowski (1986). Nevertheless, at large values of λ , say $\lambda = 0.375$ (which we studied in LR) the numerical evidence does not

exclude the possibility of rigorous ergodicity: if there are some tiny regions of stability, then they must be so small that they cannot be detected at large scales, as demonstrated in Li and Robnik (1994b), where we also show that the ergodicity may be expected for all $\lambda \geq 0.2775$. If there is some very tiny stability island (in the bounce map), then its relative area must be smaller than 5×10^{-7} .

As in LR we want to calculate and analyse the high-lying states for our billiard as high as the 100 000th state of even parity (which means the 200 000th state when counting both parities), but this time in the transitional regime of mixed-type classical dynamics such as exemplified by our billiard at $\lambda = 0.15$. In order to achieve this goal we have to use a sophisticated and powerful numerical technique and the best possible computer. We have used the Convex C3860 supercomputer and the successful method to reach our goal is our implementation of the Heller's (1991) plane-wave decomposition method described in detail in LR. While the reader is referred to LR for all technical details we should reassure him or her that many and all possible tests of numerical accuracy have been performed. The energy levels are accurate within at least 1/1000 of the mean level spacing†, and the eigenfunctions are accurate within at least 1/1000 of the average (modulus of the) probability amplitude $1/\sqrt{A}$, where $A = \pi(1 + 2\lambda^2)$ is the area of the billiard.

We have calculated more than 100 mostly consecutive even parity eigenfunctions starting from the Weyl index 100 000. By Weyl index we mean the estimated counting index of even parity states which, as a function of energy, is obtained by applying the Weyl formula with perimeter and curvature corrections; see equation (4) in our previous paper LR. Although our method allows us to accurately calculate some high-lying states it does *not* guarantee—unlike the diagonalization techniques—that we have collected all the states within a given energy interval. In fact, typically we do miss some states, especially pairs of almost degenerate states, so that even after many runs and careful checks the fraction of missing levels can be as high as 8%. Therefore this method is certainly not suitable for performing, for example, reliable level statistics, but it, nevertheless, makes it possible to watch and analyse some high states deep in the semiclassical limit. In this regard it is complementary to the conformal mapping diagonalization technique introduced by Robnik (1984) and later used by Berry and Robnik (1986), Prosen and Robnik (1993b, 1994b) and by many others. In fact we have checked the two methods against each other by verifying the accuracy of the energy levels as high as 10 000 where the double precision (16 digits) of the machine was established for not too large λ . (It is our definite experience that the numerical effort to calculate a quantum energy level increases substantially as the degree of the classical chaos increases such as, e.g. with increasing λ .) In another test of accuracy we were able to exactly (machine double precision, i.e. 16 digits) reproduce the exact eigenenergies of the analytically solvable rectangular billiard. Some of the available eigenenergies of the Heller's stadium in the literature were likewise exactly reproduced. Also, the wavefunctions for states as high as about 2000, obtained by the two different methods, have been verified to agree within the graphical resolution. Of course we have performed many other self-consistent tests of accuracy of our present method, e.g. by changing many parameters of the method, like the interior point, the boundary points and the number of plane waves, which convinced us that the claimed accuracy (see above) has been actually reached for the highest eigenstates.

In spite of these difficulties we are fairly confident that we have gathered all consecutive 36 states between the estimated Weyl index 100 008 and 100 043, whose eigenenergies as

† The step size in a single search (run) was $\frac{1}{10}$ of the mean level spacing, but we had many runs (with different parameter values such as, for example, the interior point) and each time an eigenvalue was captured we then reached the claimed accuracy.

Table 1. The eigenenergies of the corresponding eigenstates in figures 2(a), (b), 3(a), (b), 4(a) and (b). The $E = k^2$ are in the left-right, top-down order.

766 265.500	766 272.567	766 277.395
766 282.954	766 293.827	766 297.762
766 305.324	766 310.756	766 313.551
766 344.590	766 347.851	766 353.425
766 356.683	766 371.767	766 379.112
766 380.778	766 386.997	766 395.422
766 403.315	766 413.436	766 428.555
766 433.225	766 440.910	766 442.929
766 460.422	766 460.745	766 466.389
766 470.449	766 476.940	766 488.165
766 497.289	766 502.487	766 503.689
766 511.361	766 514.810	766 527.390

their unique labels are given in table 1. We believe that this is the first complete sample of consecutive high-lying eigenfunctions in the regime of mixed-type classical dynamics. It is presented in the configuration space and in the phase space in figures 2(a) and (b), 3(a) and (b) and 4(a) and (b). Now we want to discuss this phenomenological material, which we call ‘the gallery of eigenstates’.

3. The gallery of eigenstates

The wavefunctions we are looking at are the eigenfunctions of the Schrödinger equation (Helmholtz equation):

$$\Delta\Psi + E\Psi = 0 \quad \Psi = 0 \text{ at the boundary of } \mathcal{B}_\lambda \tag{2}$$

where $E = k^2$ is the eigenenergy and k the wavenumber. (So we are using units such that Planck’s constant $\hbar = 1$ and $2m = 1$, where m is the mass of the point billiard particle.)

In order to investigate the eigenstates in the quantum (Wigner) phase space we have first to define the classical phase space and the surface of section. The usual bounce map (Poincaré map) in the Birkhoff coordinates (arclength versus tangent unit velocity vector component) is not suitable for our purpose, because Ψ vanishes on the boundary. Therefore we choose the surface of section defined by $v = \text{Im}(w) = 0$. Our surface of section is now specified by the crossing point coordinate u on the abscissa versus the conjugate momentum equal to the tangential component of the velocity vector of length k with respect to the line of section $v = 0$. In figures 1(a) and (b) we show the geometry of the largest chaotic component for (a) $\lambda = 0.15$ and for (b) $\lambda = 0.2$. We do not show further details of the KAM scenario inside the stability islands in order not to obscure the structure of the phase space.

The Wigner function† (of an eigenstate $\Psi(u, v)$) defined in the full phase space (u, v, p_u, p_v) is

$$W(q, p) = \frac{1}{(2\pi)^2} \int d^2X \exp(-ip \cdot X) \Psi(q - X/2) \Psi(q + X/2) \tag{3}$$

where we have specialized to our real Ψ case, and also two degrees of freedom and $\hbar = 1$. Here $q = (u, v)$ and $p = (p_u, p_v)$. In order to compare the quantum Wigner functions with

† See, for example, Wigner (1932), Takabayasi (1954), Heller (1976, 1977) and Berry (1977a).

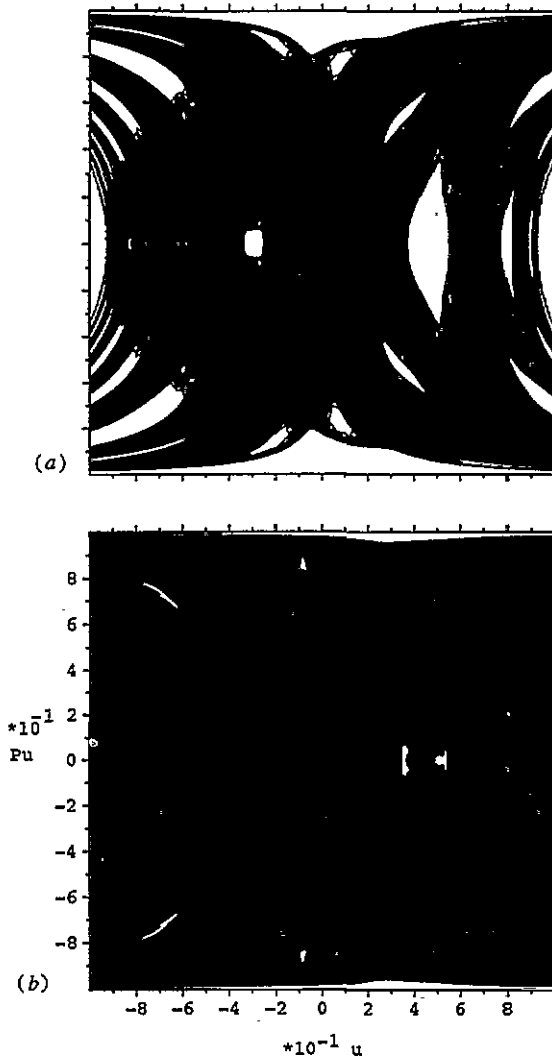


Figure 1. The classical sos of the billiard system. (a) for $\lambda = 0.15$, (b) for $\lambda = 0.2$. For the definitions see the text.

the classical Poincaré maps on the surface of section we define the following projection of (3) given as

$$\rho_{\text{sos}}(u, p_u) = \int dp_v W(u, 0, p_u, p_v) \quad (4)$$

which nicely reduces the number of integrations by one and is equal to

$$\rho_{\text{sos}}(u, p_u) = \frac{1}{2\pi} \int dx \exp(ixp_u) \Psi(u + \frac{1}{2}x, 0) \Psi(u - \frac{1}{2}x, 0). \quad (5)$$

As is well known the Wigner function and its projections are not positive definite and indeed one typically finds small and inconvenient but nevertheless physical oscillations around zero which seriously obscure the main structural features. Therefore in order to compare the

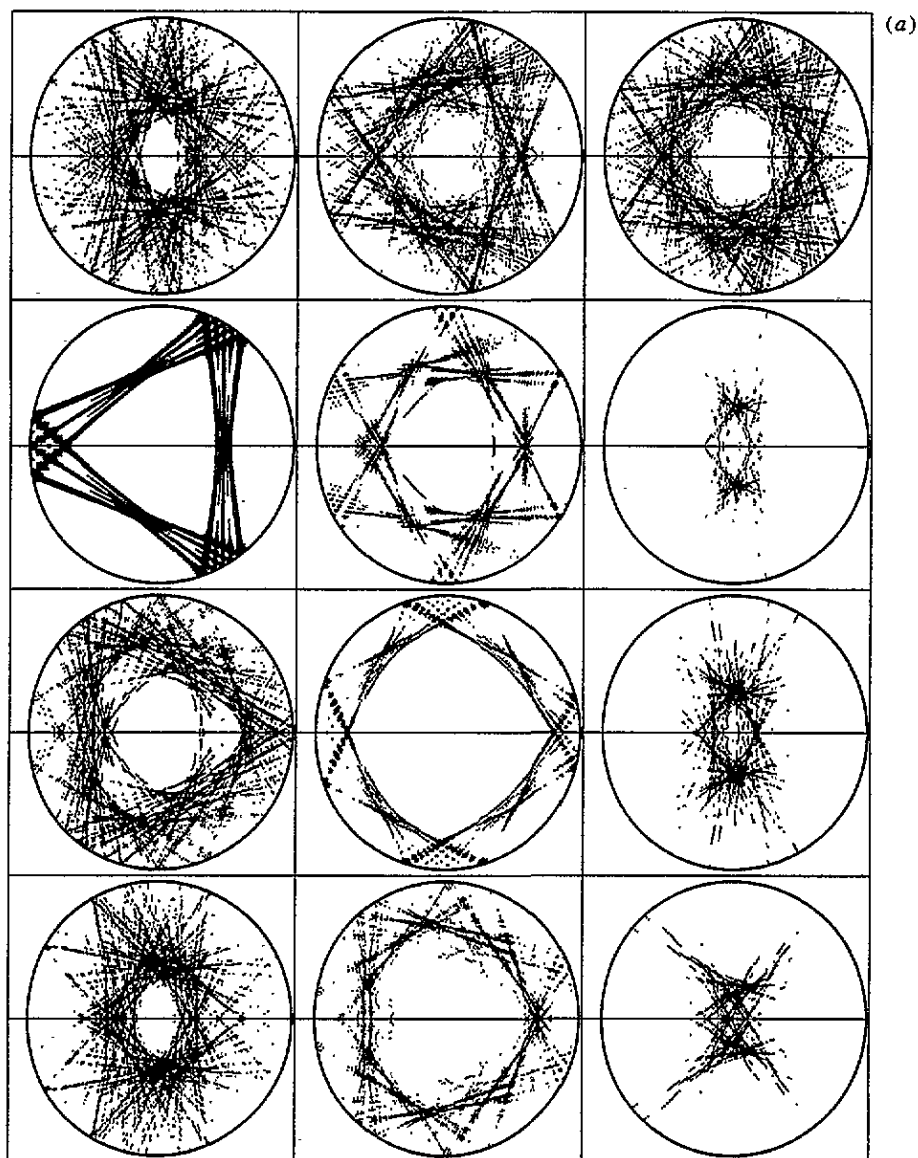


Figure 2. The first 12 states from the gallery of eigenstates. The eigenfunctions in configuration space (a) and the corresponding smoothed Wigner function ρ_{SOS} (b). In (a) the contours are plotted at eight equally spaced steps between zero and the maximum value. In (b) the contours start from $\frac{1}{8}$ with the step size $\frac{1}{8}$. The abscissa in (b) is just the coordinate on the line of section whilst the ordinate goes from $-\sqrt{E}$ to \sqrt{E} , where E is the eigenenergy of the given state. Please notice that the classically allowed value of p_u is within the interval $[-\sqrt{E}, \sqrt{E}]$. For labelling of individual plots see the text.

classical and quantal phase-space structure it is advisable to smooth the Wigner function or its projections (5) by a normalized Gaussian kernel with a suitably adapted dispersion. Such a procedure has been introduced and used in Takahashi (1989, Leboeuf and Saraceno (1990), Heller (1991), Prosen and Robnik (1993c), which is a Husimi-type representation

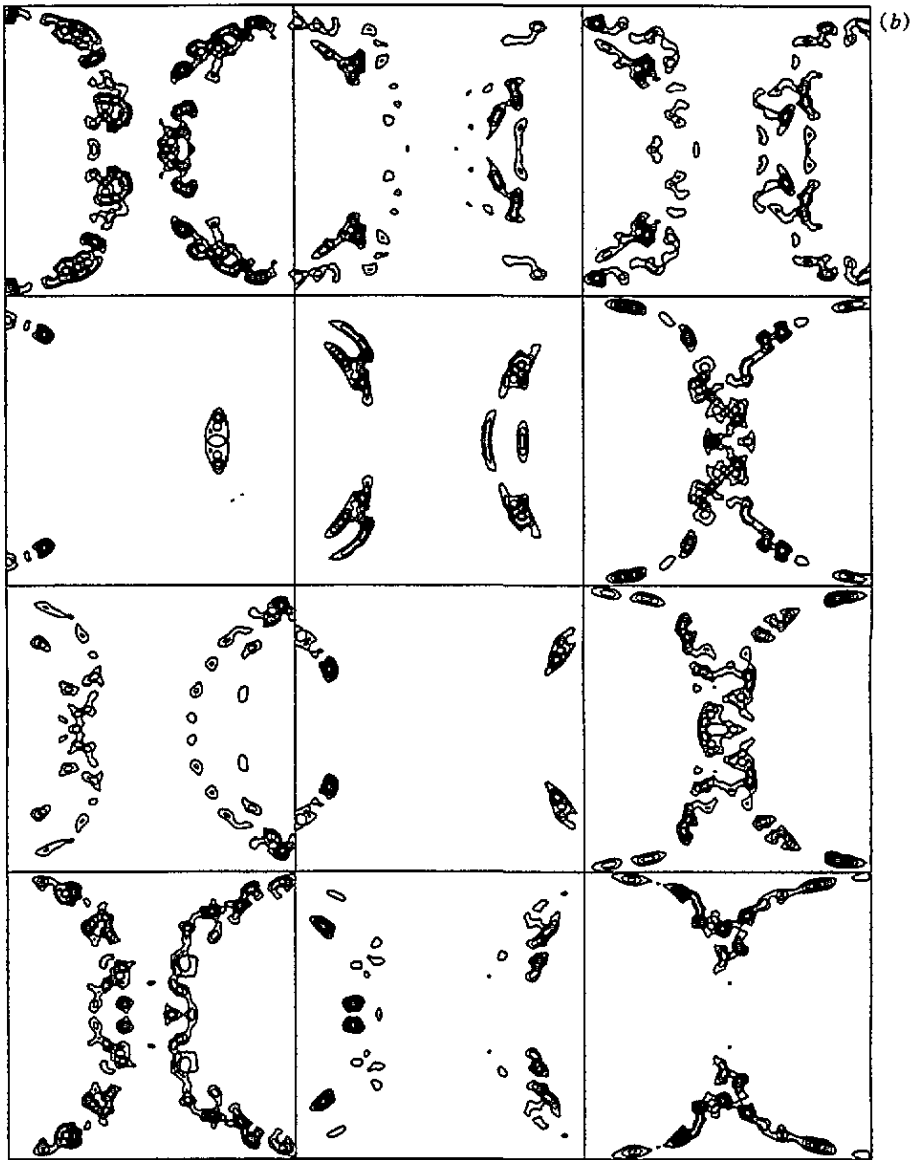


Figure 2. Continued.

but the effective area of our Gaussian kernel will be smaller than 2π . To be more specific, we should clearly state the size of the effective action area $h_{eff} = 2\pi/\sqrt{E}$ in all our phase-space plots, in particular, figures 2–4(b), is about $\frac{1}{400}$ of the entire SOS area. The area of the circle at the half maximum of our smoothing Gaussian is about nine times smaller than h_{eff} .

In discussing our gallery of eigenstates we shall use the following labelling of individual plots in figures 2–4: (nx, i, j) identifies the plot in the i th row and j th column (just the standard matrix element notation) of figure nx , where nx denotes the number of the given figure, so it could be 2(a)–4(b). Thus for example $(3a, 3, 2)$ is the second plot in the third

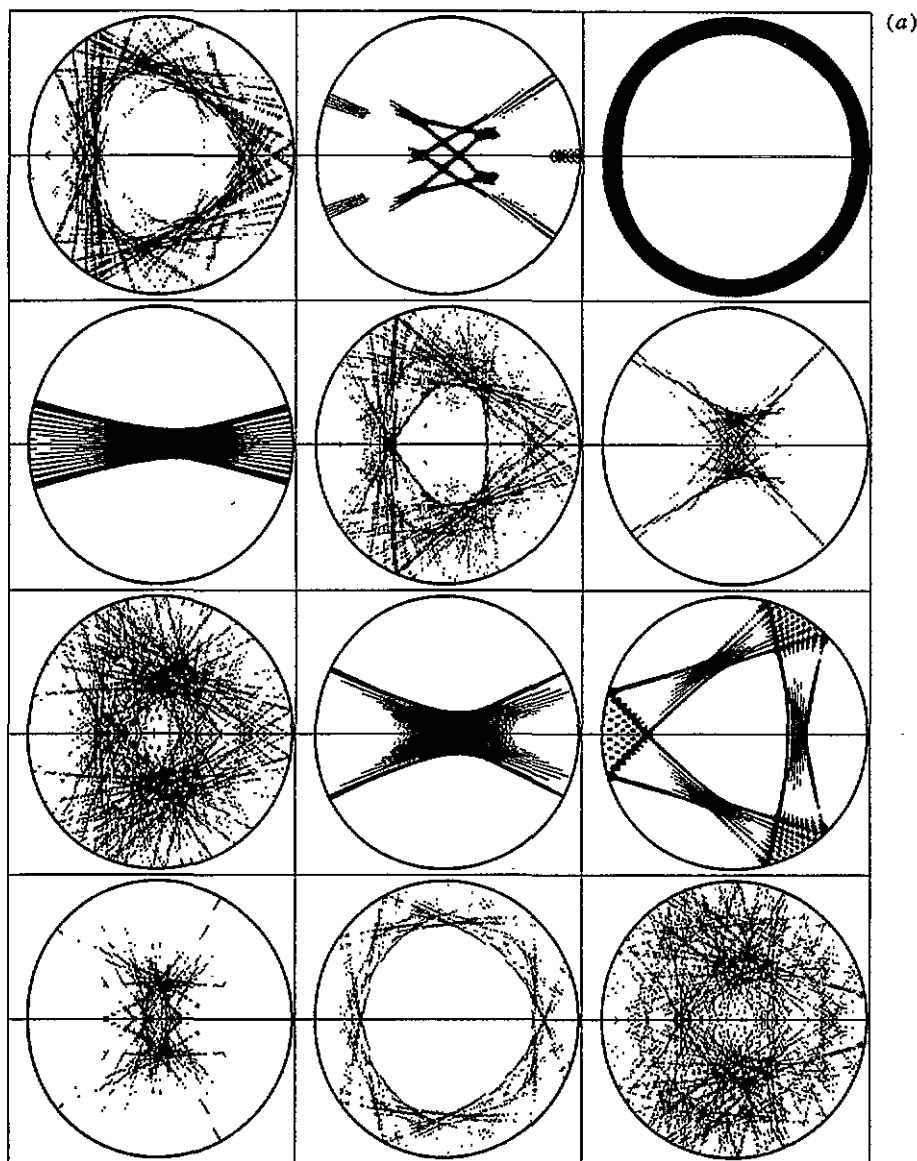


Figure 3. The same as figure 2 but for the second 12 states from the gallery of eigenstates.

row of figure 3(a).

In figures 2(a) and (b) when the plots in 2(b) are compared with the classical plot in figure 1(a) we immediately realize that all states should be classified as irregular (chaotic), because their smoothed Wigner functions are concentrated inside the classical chaotic region, except for two eigenstates ($2a-b, 2, 1$) and ($2a-b, 3, 2$). The former of these two regular eigenstates is clearly associated with the corresponding quantized classical invariant torus, shown in figure 6(a) together with two other regular states. This observation is based on the comparison of the geometries by eye and could be made quantitative by performing the torus quantization. In our survey of more than 100 states we have seen at least five

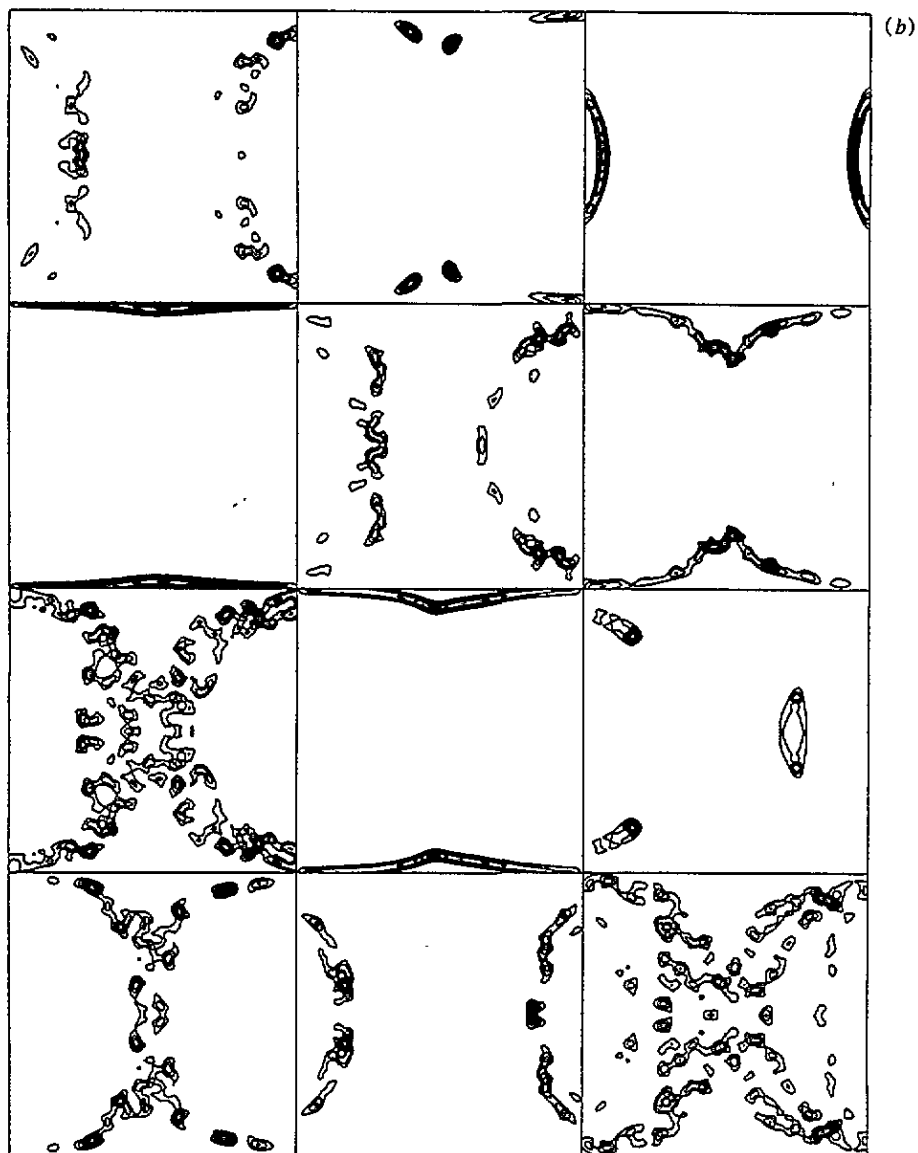


Figure 3. Continued.

such similar states on a classical invariant torus with winding number close to three. The second regular state $(2a-b, 3, 2)$ is also 'living' on a classical invariant torus but we do not show that. As for the vast majority of chaotic states we should make the preliminary general comment that they are typically strongly localized inside the classically available chaotic region which is immediately obvious in the phase-space plots of figure 2(b) but not necessarily in the configuration space plots of figure 2(a). Structurally similar localized chaotic eigenstates are $(2a, 1, 1)$, $(2a, 1, 3)$ and $(2a, 4, 1)$ which is also uncovered in the phase space of figure 2(b). Another set of similar structure are $(2a, 2, 3)$, $(2a, 3, 3)$ and $(2a, 4, 3)$ which are concentrated in the centre of the chaotic region. The next class

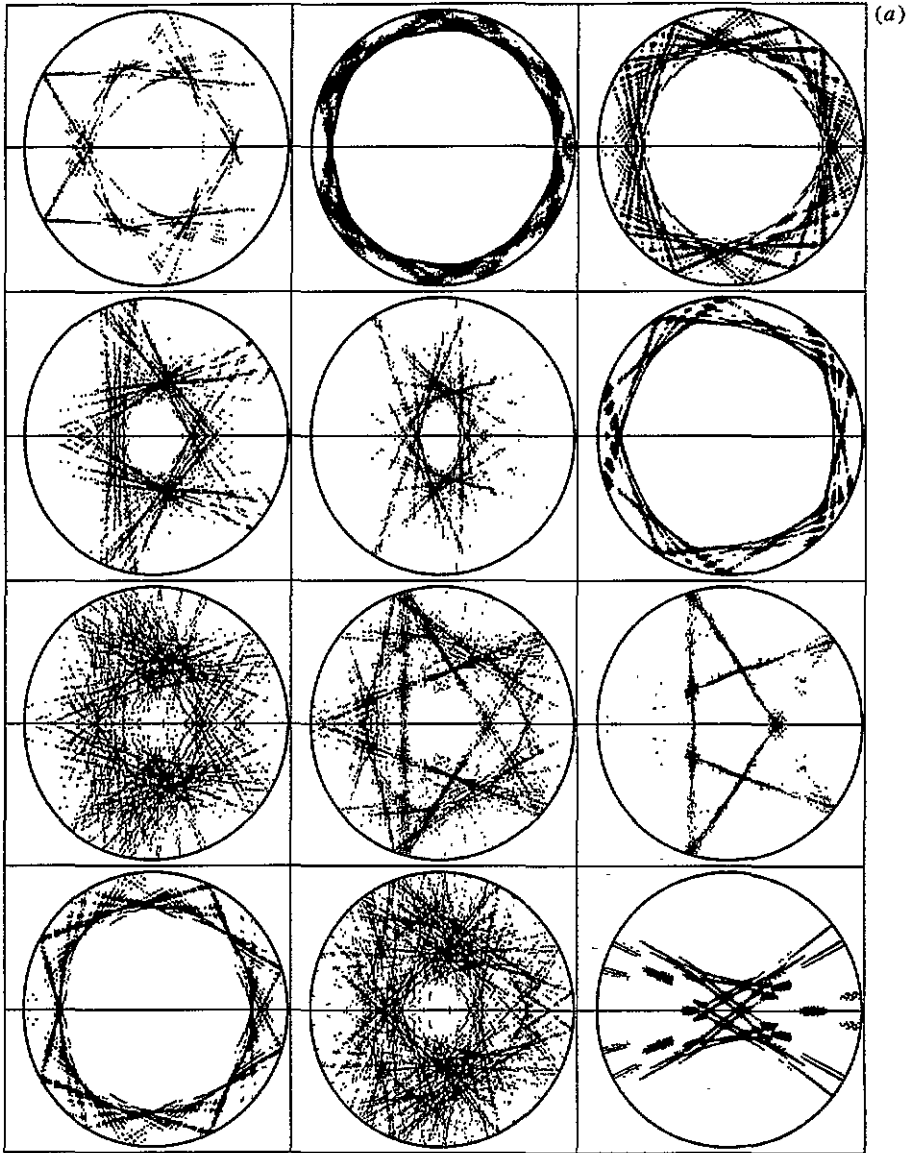


Figure 4. The same as figure 2 but for the last 12 states from the gallery of eigenstates.

of similar states are $(2a, 1, 2)$ and $(2a, 3, 1)$. The chaotic state $(2a, 2, 2)$ is localized at the border of stability islands as is seen in $(2b, 2, 2)$ compared with figure 1(a). The remaining state $(2a-b, 4, 2)$ of figures 2(a) and (b) is strongly localized in a region where classical dynamics has been verified to be chaotic but exhibiting very slow diffusion. This quantal localization therefore has a classical origin, because, as can be easily verified, the quantum break time is much shorter than the classical diffusion time. The quantum break time $t_{break} = \hbar/\Delta E$ is quite generally defined in terms of the (locally) mean level spacing ΔE (Chirikov *et al* 1981).

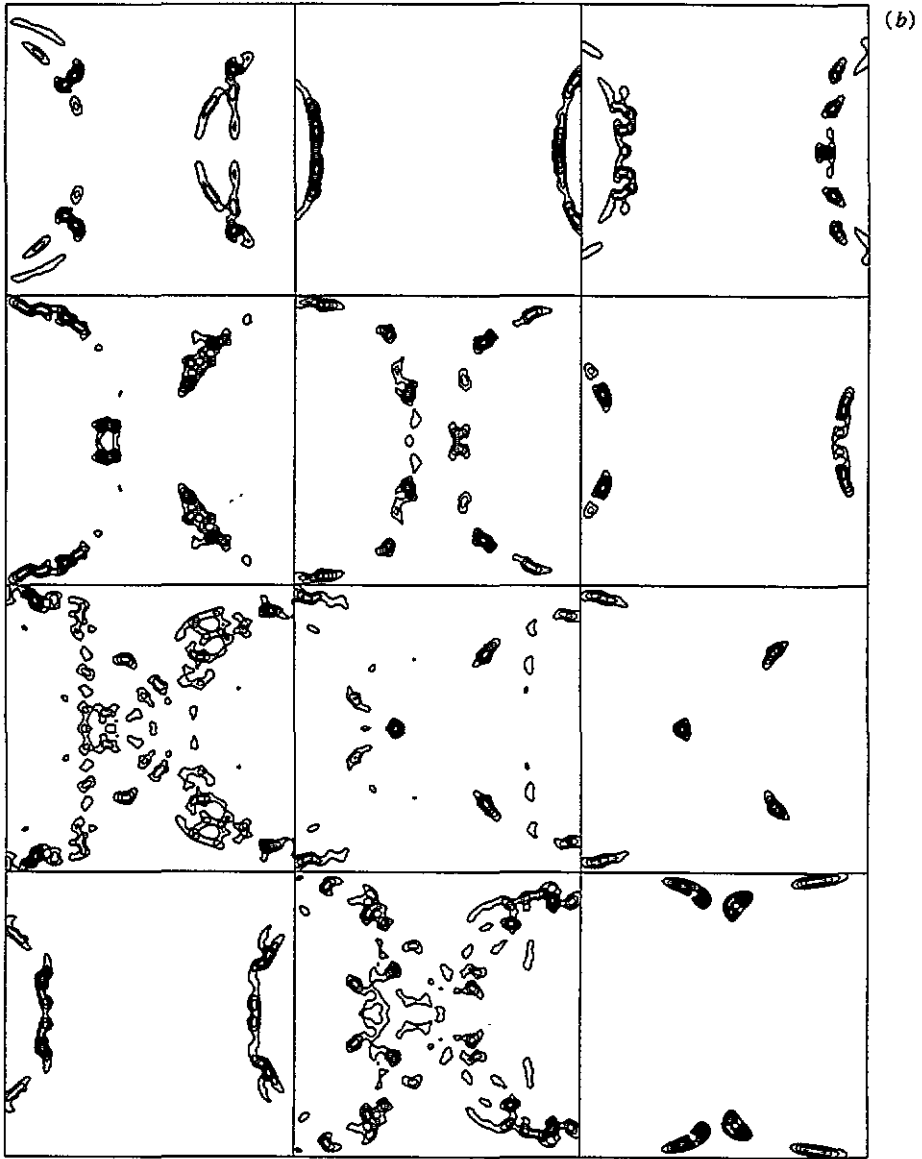


Figure 4. Continued.

In figures 3(a) and (b) we identify five regular states: three of them, namely $(3a-b, 1, 2)$, $(3a-b, 2, 1)$ and $(3a-b, 3, 2)$, are bouncing-ball-type in the region close to the horizontal diametral periodic orbit, all of them being associated with a classical quantized invariant torus: a quasiperiodic orbit on such a torus is shown in figure 6(b) and it captures especially the structure of the state $(3a, 2, 1)$; the state $(3a-b, 1, 3)$ is a whispering gallery mode (Lazutkin 1981, 1991, Keller and Rubinow 1960, Walker 1978): unfortunately, its oscillatory structure having 10 nodal lines ('circles') is not graphically resolved; the state $(3a-b, 3, 3)$ is similar to $(2a-b, 2, 1)$ and thus also 'lives' on the invariant torus close to period 3. Further we have three sets of similar chaotic states: $(3a-b, 1, 1)$ and $(3a-b, 2,$

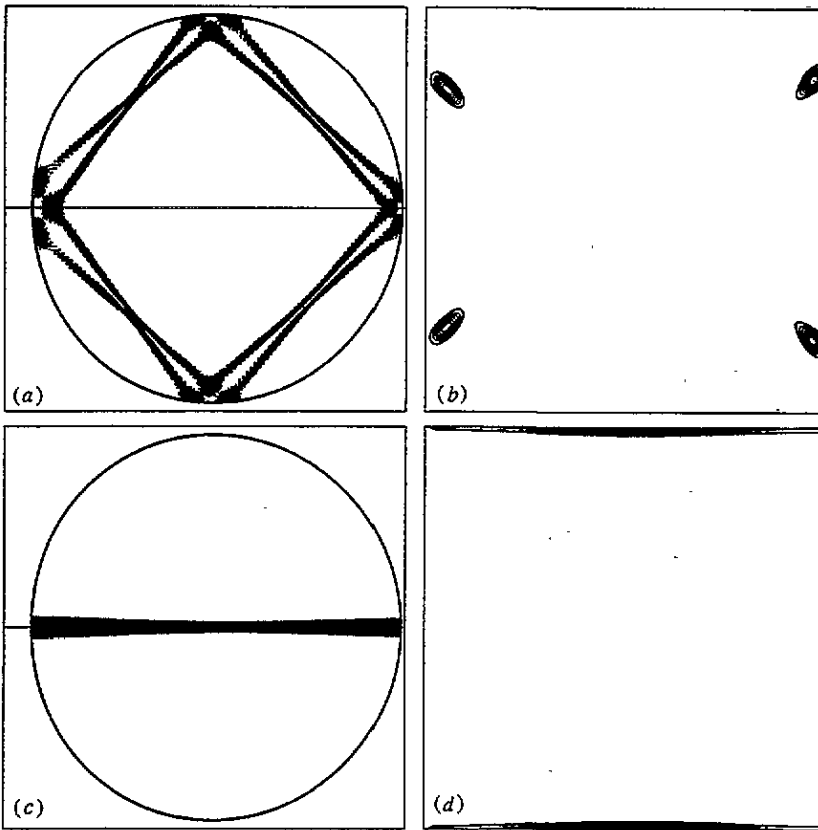


Figure 5. Two examples of regular states in configuration space (a), (c) and in phase space (b), (d). The energy of the top one is 766 536.529 and the bottom one is 766 569.685.

2); then the two centrally localized states $(3a-b, 2, 3)$ and $(3a-b, 4, 1)$; and finally, the least localized chaotic states $(3a-b, 3, 1)$ and $(3a-b, 4, 3)$. Notice that as the degree of chaoticity increases from the former to the latter in the corresponding phase-space plots $(3b, 3, 1)$ and $(3b, 4, 3)$ we observe the tendency towards more extended chaotic states.

We should mention that an attempt to semiclassically quantize the most regular state $(3a-b, 1, 3)$, which is a whispering gallery mode, in the Keller–Rubinow (1960) formulation, resulted in a semiclassical energy eigenvalue which differs from the exact one by about 5% of the mean level spacing. This experience is not unexpected and conforms with the demonstration by Prosen and Robnik (1993a), where they argue that the semiclassical methods (at the level of torus quantization or Gutzwiller theory) generally fail to predict the individual energy levels within a vanishing fraction of the mean level spacing even in the semiclassical limit when $\hbar \rightarrow 0$. For related developments see Boasman (1992).

In figures 4(a) and (b) we have four examples of regular states: $(4a-b, 2, 1)$ which is marginally regular (see the classical plot in figure 1(a)), and $(4a-b, 3, 3)$ which, in fact, is an excellent example of a regular state, ‘living’ on a thin invariant torus around a classical periodic orbit of period 5; $(4a-b, 4, 3)$ which again is a bouncing-ball-type state around the horizontal diametral periodic orbit, and $(4a-b, 2, 3)$ which is an example

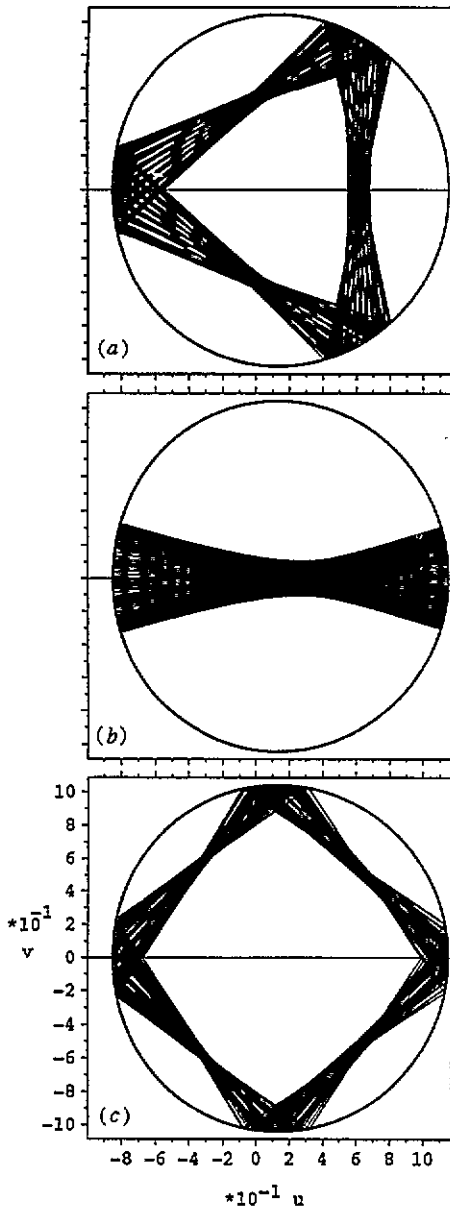


Figure 6. A quasiperiodic classical orbit on the invariant torus supporting a regular eigenstate: $(2a-b, 2, 1)$ in (a); $(3a-b, 2, 1)$ in (b) and figures 5(a) and (b) in (c).

of a 'survived' whispering gallery mode. We should stress that $(4b, 4, 3)$ lives on the torus which is close to but disjoint from the torus of the bouncing ball modes. Regarding $(4b, 2, 3)$ a similar comment applies. In the plots $(4a-b, 3, 2)$ we uncover a mixed-type state which, however, is close to the regular state $(4a-b, 3, 3)$. All the remaining states are chaotic but some of them are strongly localized like $(4a-b, 1, 1)$, $(4a-b, 1, 2)$, $(4a-b, 1, 3)$, $(4a-b, 2, 2)$ and $(4a-b, 4, 1)$: all of them are localized in the region of the phase space where classical dynamics is chaotic but very slowly diffusive. The remaining two eigenstates $(4a-b, 3, 1)$ and $(4a-b, 4, 2)$ are rather extended chaotic states.

4. Further analysis of some representative eigenstates

Apart from the states displayed in the gallery of eigenstates we have inspected many more (more than 100) states in configuration and in phase space. Now we want to show and discuss some of them, belonging to various classes. In figure 5(a) we give an example of a regular state which semiclassically would be described as a thin quantized torus close to the classical periodic orbit of period 4, as is evident in the phase-space plot of the same eigenstate in figure 5(b). The classical quasiperiodic orbit associated with this state is shown in figure 6(c). In this plot we see a signature of classical probability density explaining the structure in figure 5(a). However, having in mind that the de Broglie wavelength is about $\frac{1}{278}$ of the horizontal diameter of the billiard, one recognizes that there is a phenomenon of strong destructive interference which leads to the gaps of strongly depressed probability density as wide as 10–15 de Broglie wavelengths. Another example of a regular state close to the stable classical periodic orbit of period 2 is shown in figures 5(c) and (d): again it is a quantum state 'living' on a thin quantized torus around the diametral periodic orbit.

In figure 7(a) we show an interesting example of a scarred chaotic state. At first glance it has the appearance of a regular state but in reality it is definitely irregular but strongly localized in the vicinity of the supporting *unstable* classical periodic orbit of period 7. This

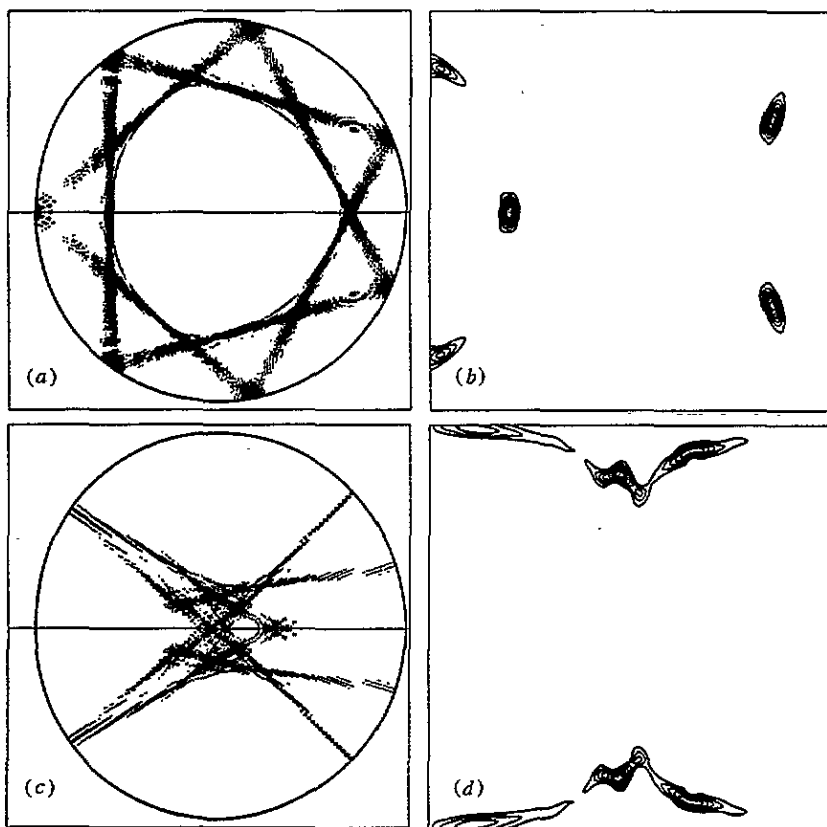


Figure 7. Two examples of eigenstates in configuration space (a), (c) and in phase-space (b), (d). The energy of the top one is 766 718.836 and the bottom one is 766 940.785. (a), (b) is a scarred chaotic state whereas (c), (d) is a mixed-type state.

is obvious when figure 7(b) is compared with figure 1(a).

In figure 7(c) we see an example of a mixed-type state in the sense that in the phase space (in figure 7(d)) it is concentrated partially both on a regular and on a chaotic region. Such mixed-type states become more and more rare in the semiclassical limit when $\hbar \rightarrow 0$ or equivalently when $E \rightarrow \infty$. This observation which we have checked phenomenologically in our numerical experiments supports the correctness of Percival's (1973) classification of semiclassical states in regular and irregular ones.

After our qualitative review of the variety of eigenstates we want to give some quantitative statistical characterization. A similar analysis of the probability amplitude distribution of strongly chaotic eigenstates (at $\lambda = 0.375$) has been published in LR, where the appropriateness of the Gaussian random model for the probability amplitude distribution $P(\Psi)$ has been confirmed. Similar results have been published in Aurich and Steiner (1993). $P(\Psi)$ is the probability density of finding an amplitude Ψ inside an infinitesimal interval $(\Psi, \Psi + d\Psi)$. Of course, in regular states or strongly localized chaotic states there are large regions in configuration space where the probability density almost vanishes, and that gives rise to a delta spike in the corresponding $P(\Psi)$ at $\Psi = 0$. Therefore in the transition region of states going from localized to extended chaotic we shall see a gradual decrease of the central delta spike and the tendency of $P(\Psi)$ towards the Gaussian random model

$$P(\Psi) = \frac{1}{\sqrt{2\pi}\sigma} \exp\left\{-\frac{\Psi^2}{2\sigma^2}\right\} \quad (6)$$

where according to PUSC $\sigma^2 = 1/\mathcal{A} = 1/(\pi(1 + 2\lambda^2))$. In figure 8 we show such a transition for two states from the gallery of eigenstates, namely (4a, 1, 3) and (2a, 1, 2),

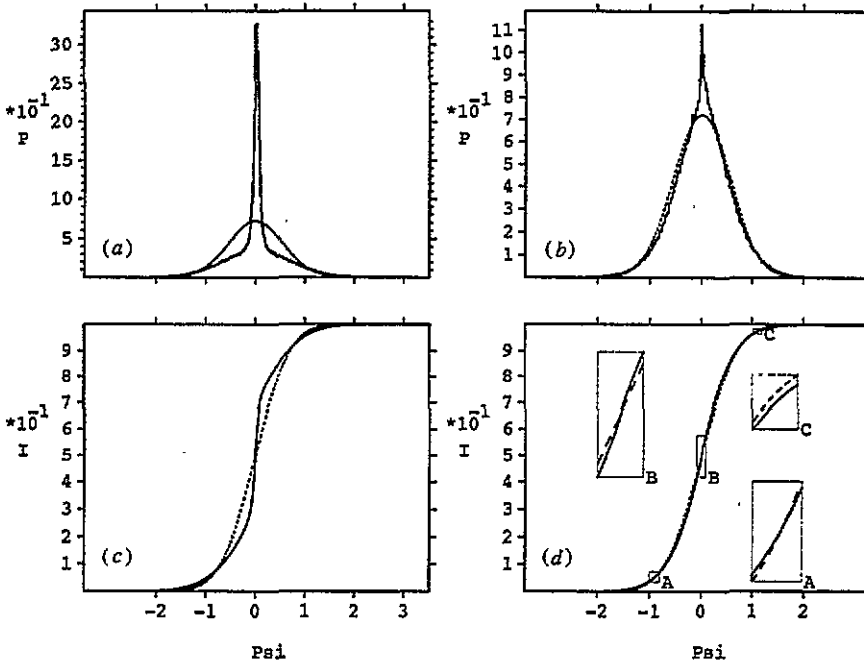


Figure 8. The statistics of two eigenstates (4a-b, 1, 3) in (a), (c) and (2a-b, 1, 2) in (b), (d). In (a), (b) we plot the amplitude probability density $P(\Psi)$ and in (c), (d) the cumulative distribution $I(\Psi)$. The numerical data are shown as full curves and the theoretical Gaussian as a broken curve.

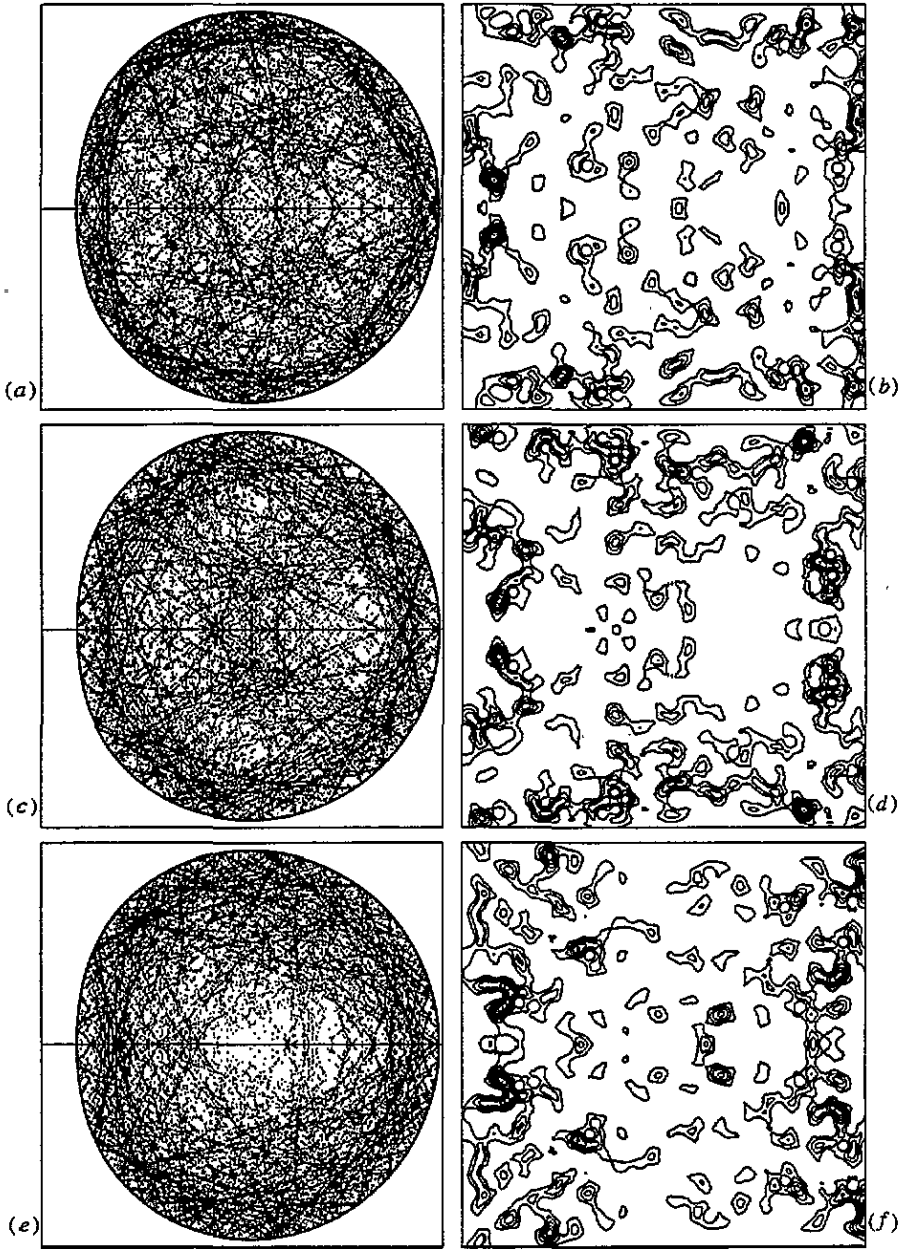


Figure 9. Three examples of extended chaotic eigenstates for $\lambda = 0.2$ in configuration space (a), (c), (e) and in phase space (b), (d), (f). The energies are: 741 511.898 in (a), (b); 741 525.937 in (c), (d); 741 549.855 in (e), (f). The Weyl index of these states is 100 017, 100 019 and 100 022, respectively.

in figures 8(a)–(d), correspondingly. The plots 8(a) and (b) are $P(\Psi)$ plots obtained by covering the configuration space with about 250 000 grid points. In figures 8(c) and (d) we show the corresponding cumulative distributions $I(\Psi) = \int_{-\infty}^{\Psi} dx P(x)$. The former of these two states is clearly strongly localized chaotic whereas the latter is already surprisingly

close to the Gaussian random model even though it is not yet a completely extended chaotic state.

In order to illustrate the importance of the classical diffusion in the classical chaotic regions of the phase space for the quantum localization of the chaotic eigenstates we should remind the reader that quite generally the quantum evolution follows the classical dynamics up to the break time, which is by definition equal to $t_{break} = \hbar/\Delta E$ (Chirikov *et al* 1981), where ΔE is the mean energy level spacing. After the break time the quantum diffusion generally stops resulting in a localization due to quantum interference effects. (The reason is that in the quantum time evolution of a purely bound system the discreteness of the spectrum of the quantum evolution operator starts to manifest itself only at times larger than the break time.) If the classical diffusion time is much shorter than the break time then the quantum evolution of an initially localized state can reach full extendedness before the break time. We have verified that this inequality is indeed strongly violated at $\lambda = 0.15$. Therefore, for this shape of the billiard domain the vast majority of chaotic states are strongly localized as demonstrated in the gallery of eigenstates of section 3. In order to show the approach to the extended chaotic regime, in figures 9(a)–(f) we show three quite typical chaotic eigenstates for the billiard at $\lambda = 0.2$ all of which are fully extended chaotic as is clearly evident when the phase-space plots 9(b), (d) and (f) are compared with figure 1(b). Of course, we have verified that here the break time is now much larger than the classical diffusion time, so that the extendedness is reached before the break time.

5. Discussions and conclusions

We believe that our present work reveals the structural richness of eigenfunctions in quantum systems deep in the semiclassical regime having mixed classical dynamics. In surveying more than 100 high-lying states around and above the 100 000th state of even parity we have persuasively demonstrated that Percival's (1973) classification into regular and irregular states works well. While regular states are associated with some quantized classical invariant tori the chaotic states do not necessarily occupy the entire classically accessible chaotic region, but can be instead strongly localized especially in cases of slow classical diffusion where the break time is shorter than the classical diffusion time. This qualitative observation is demonstrated in sections 3 and 4, where we also show the approach to the uniform extendedness in chaotic eigenstates when the above-mentioned inequality is reversed. Thereby we have also clearly verified the validity of the principle of the uniform semiclassical condensation outlined in the introduction. A more quantitative study of this aspect would require us to describe the localization or extendedness at sufficiently many billiard shapes such that we would densely cover the transition from strong localization characterized by the inequality $t_{break} \ll t_{diff}$ to full extendedness characterized by $t_{break} \gg t_{diff}$, where t_{diff} is the classical diffusion time. Unfortunately, the present day semiclassical methods and approximations are not yet good enough to predict (the eigenvalue and the structure of) the individual eigenstates, cf Prosen and Robnik (1993a). Nevertheless, a lot of the structure of the eigenfunctions can be associated and qualitatively explained *a posteriori* by semiclassical quantization which thus provides the understanding of the various classes of generic behaviour, such as the regular and irregular states, and the further subclassification of the latter into localized, scarred and extended states.

We feel that the present numerical work is a challenge to improve the semiclassical methods to the extent that they would have the potential of predicting the individual states. The first step in this direction has recently been undertaken by Gaspard and Alonso (1993) where they have worked out the corrections to the leading term embodied in the Gutzwiller

trace formula. Further numerical and theoretical work should be done to improve our knowledge about the statistical properties of the eigenstates. For example, one could count the fraction of regular states within a sufficiently large block of consecutive high-lying eigenstates, which according to the rigorous theory of Lazutkin (1981, 1991) concerning the semiclassical asymptotics should be precisely equal to the fractional volume of the regular components in the classical phase space[†]. This fact is, for example, one major assumption in the Berry–Robnik (1984) theory. For this to end we need to have a better numerical method with no missing of eigenstates ensuring significant statistics, which at present we do not (yet) possess for such high-lying states, whereas for low states (say, up to 10 000) we certainly could use our conformal diagonalization technique (see, for example, Prosen and Robnik 1993c) but then we are probably not sufficiently far in the semiclassical limit for an unambiguous classification in regular and irregular states. This is studied and discussed in detail in our next paper (Li and Robnik 1994c,d), where we successfully separate regular and irregular energy levels, using the dynamical criterion of comparing the classical and quantal phase-space plots on SOS, and investigate the level statistics of the two level sequences separately. But there is still much more work to be done especially such as a more quantitative analysis on points (i)–(iii) raised and listed in the abstract.

Acknowledgments

We thank Tomaž Prosen for a few computer programs and assistance in using them. One of us (MR) acknowledges stimulating discussions with Oriol Bohigas, Boris V Chirikov, Marcos Saraceno and Hans A Weidenmüller. Finally we thank the second of the two referees for the careful, constructive and critical report. The financial support by the Ministry of Science and Technology of the Republic of Slovenia is gratefully acknowledged.

References

- Aurich R, Bolte J and Steiner F 1994 *Phys. Rev. Lett.* **73** 1356
 Aurich R and Steiner F 1993 *Physica* **64D** 185
 Berry M V 1977a *Phil. Trans. R. Soc.* **287** 237
 —1977b *J. Phys. A: Math. Gen.* **10** 2083
 —1983 *Chaotic Behaviour of Deterministic Systems (Proc. NATO ASI Les Houches Summer School)* ed G Iooss, R H G Helleman and R Stora (Amsterdam: Elsevier) p 171
 —1985 *Proc. R. Soc. A* **400** 229
 —1989 *Proc. R. Soc. A* **423** 219
 Berry M V and Robnik M 1984 *J. Phys. A: Math. Gen.* **17** 2413
 —1986 *J. Phys. A: Math. Gen.* **19** 649
 Boasman P A 1994 *Nonlinearity* **7** 485
 Bohigas O 1991 *Chaos and Quantum Systems (Proc. NATO ASI Les Houches Summer School)* ed M-J Giannoni, A Voros and J Zinn-Justin (Amsterdam: Elsevier) p 87
 Bogomolny E B 1988 *Physica* **31D** 169
 Bruus H and Stone A D 1994 *Phys. Rev. B* **50** 18 275
 Casati G, Guarneri I and Smilansky U (eds) 1993 *Quantum Chaos* (Amsterdam: North-Holland)
 Chirikov B V, Shepelyansky D L and Izrailev F M 1981 *Sov. Sci. Rev. C* **2** 209
 Frisk H 1990 *Nordita Preprint*
 Gaspard P and Alonso D 1993 *Phys. Rev. E* **47** R3468
 Giannoni M-J, Voros J and Zinn-Justin (eds) 1991 *Chaos and Quantum Systems* (Amsterdam: North-Holland)

[†] Our gallery of 36 consecutive eigenstates is the only block of states for which we are fairly confident that there are no missing states. 11 of these eigenstates are regular so that their relative fraction is 30.6% which, surprisingly, is not too far from the classical fractional volume of the regular component in the classical phase space which according to Prosen and Robnik (1993c) is equal to 36%.

- Gutzwiller M C 1990 *Chaos in Classical and Quantum Mechanics* (New York: Springer)
- Hayli A, Dumont T, Moulin-Ollagier J and Strelcyn J M 1987 *J. Phys. A: Math. Gen.* **20** 3237
- Heller E J 1976 *J. Chem. Phys.* **65** 1289
- 1977 *J. Chem. Phys.* **67** 3339
- 1984 *Phys. Rev. Lett.* **53** 1515
- 1991 *Chaos and Quantum Systems (Proc. NATO ASI Les Houches Summer School)* ed M-J Giannoni, A Voros and J Zinn-Justin (Amsterdam: Elsevier) p 547
- Keller J B and Rubinow S I *Ann. Phys., NY* **10** 303
- Lazutkin V F 1981 *The Convex Billiard and the Eigenfunctions of the Laplace Operator (Leningrad: University Press)* (in Russian)
- 1991 *KAM Theory and Semiclassical Approximations to Eigenfunctions* (Heidelberg: Springer)
- Leboeuf P and Saraceno M 1990 *J. Phys. A: Math. Gen.* **23** 1745
- Li Baowen and Robnik M 1994a *J. Phys. A: Math. Gen.* **27** 5509
- 1994b *J. Phys. A: Math. Gen.* to be submitted
- 1994c *Preprint CAMTP/94-10* (submitted to *J. Phys. A: Math. Gen.*)
- 1994d *Preprint CAMTP/94-11* to be submitted
- Markarian R 1993 *Nonlinearity* **6** 819
- Mather J N 1982 *Ergodic Theory and Dynamical Systems* **2** 3
- 1988 *Ergodic Theory and Dynamical Systems* **8** 199
- Percival I C 1973 *J. Phys. B: At. Mol. Phys.* **6** L229
- Prosen T and Robnik M 1993a *J. Phys. A: Math. Gen.* **26** L37
- 1993b *J. Phys. A: Math. Gen.* **26** 5365
- 1993c *J. Phys. A: Math. Gen.* **26** 2371
- 1994a *J. Phys. A: Math. Gen.* **27** L459
- 1994b *J. Phys. A: Math. Gen.* **27** 8059
- Provost D and Baranger M 1993 *Phys. Rev. Lett.* **71** 662
- Robnik M 1983 *J. Phys. A: Math. Gen.* **16** 3971
- 1984 *J. Phys. A: Math. Gen.* **17** 1049
- 1988 *Atomic Spectra and Collisions in External Fields* ed K T Taylor, M H Nayfeh and C W Clark (New York: Plenum) pp 265–74
- 1994 *J. Phys. Soc. Japan Suppl.* **63** 131
- Shnirelman A L 1979 *Usp. Mat. Nauk* **29** 181
- Steiner F 1994 *Quantum chaos Schlaglichter der Forschung (Zum 75 Jahrestag der Universität Hamburg 1994)* ed R Ansorge Festschrift published on the occasion of the 75th anniversary of the University of Hamburg (Berlin: Reimer) p 543
- Stone A D and Bruus H 1993a *Physica* **189B** 43
- 1993b *Surface Sci.* **305** 490
- Szerefi T, Lefebvre J H and Goodings D A 1994 *Nonlinearity* **7** 1463
- Takabayasi T 1954 *Prog. Theor. Phys. (Kyoto)* **11** 341
- Takahashi K 1989 *Prog. Theor. Phys. Suppl. (Kyoto)* **98** 109
- Voros A 1979 *Lecture Notes in Physics* **93** 326
- Walker J 1978 *Sci. Am.* **239** 146
- Wojtkowski M 1986 *Commun. Math. Phys.* **105** 391